15 Niwa H, Yamamura K, Miyazaki J. Efficient selection for high-expression transfectants with a novel eukaryotic vector. Gene 1991; 108: 193-199.

16 Tanemura K, Ogura A, Cheong C et al. Dynamic rearrangement of telomeres during spermatogenesis in mice. Dev Biol 2005; 281: 196-207.

17 Sawano A, Hama H, Saito N et al. Multicolor imaging of Ca(2+) and protein kinase C signals using novel epifluorescence microscopy. Biophys J 2002; 82: 1076-1085.

18 Okada S, Nakamura M, Mikami Y et al. Blockade of interleukin-6 receptor suppresses reactive astrogliosis and ameliorates functional recovery inexperimental spinal cord injury. J Neurosci Res 2004; 76: 265-276.

19 Crabtree GR, Olson EN. NFAT signaling: choreographing the social lives of cells. Cell 2002; 109: S67-S79.

20 Tanabe Y, William C, Jessell TM. Specification of motor neuron identity by MNR2 homeodomain protein. Cell 1998; 95: 67-80.

21 Tsuchida T, Ensini M, Morton SB et al. Topographic organization of embryonic motor neurons defined by expression of LIM homeobox genes. Cell 1994; 79: 957-970.

22 Beattie MS, Bresnahan JC, Komon J et al. Endogenous repair after spinal cord contusion injuries in the rat. Exp Neurol 1997; 148: 453-463.

23 Johansson CB, Momma S, Clarke DL et al. Identification of a neural stem cell in the adult mammalian central nervous system. Cell 1999; 96: 25-34.

24 Johansson CB, Lothian C, Molin M et al. Nestin enhancer requirements for expression in normal and injured adult CNS. J Neurosci Res 2002; 69: 784-794.

25 Nakamura M, Bregman BS. Difference in neurotrophic factor gene expression profiles between neonate and adult rat spinal cord after injury. Exp Neurol 2001; 169: 407-415.

26 Okano H. The stem cell biology of the central nervous system. J Neurosci Res 2002; 69: 698-707.

27 Nakamura M, Houghtling RA, MacArthur L et al. Differences in cytokine expression profile between acute and secondary injury in adult rat spinal cord. Exp Neurol 2003; 184: 313-325.

28 Okano H, Ogawa Y, Nakamura M et al. Transplantation of neural stem cells into the spinal cord after injury. Semin Cell Dev Biol 2003; 379: 1-8.

29 Cohan CS. Frequency-dependent and cell-specific effects of electrical activity on growth cone movements of cultured Helisoma neurons. J Neurobiol 1990; 21: 400-413.

30 Nakae H. Morphological differentiation of rat pheochromocytoma cells (PC12 cells) by electric stimulation. Brain Res 1991; 558: 348-352.

31 Manivannan S, Terakawa S.Rapid sprouting of filopodia in nerve terminals of chromaffin cells, PC12 cells, and dorsal root neurons induced by electrical stimulation. J Neurosci 1994; 14: 5917-5928.

32 Aniksztejn L, Demarque M, Morozov,Y Ben-Ari Y, Represa A. Recurrent CA1 collateral axons in developing rat hippocampus. Brain Res 2001; 913:195-200.

33 McCraig CD, Rajnicel AM, Song B, Zhao M. Has electrical growth cone guidance found its potential? Trends Neurosci 2002; 25: 354-359.

34 Kessel M, Gruss P. Homeotic transformations of murine vertebrae and concomitant alteration of *Hox* codes induced by retinoic acid. Cell 1991; 67: 89-104.

35 Ogawa Y, Sawamoto K, Miyata T et al. Transplantation of in vitro expanded fetal neural progenitor cells results in neurogenesis and functional recovery after spinal cord contusion injury in adult rats. J Neurosci Res 2002; 69: 925-933.

36 Pandur P, Maurus D, Kuhl M. Increasingly complex: new players enter the Wnt signaling network. BioEssays 2002; 24: 881-884.

37 Kuhl M, Sheldahl LC, Malbon CC et al. Ca^{2+}/Calmodulin-dependent protein kinase II is stimulated by Wnt and Frizzled homologs and promotes ventral cell fates in *Xenopus*. J Biol Chem 2000; 275: 12701-12711.

38 Yamada M, Nakanishi K, Ohba S et al. Brain-Derived Neurotrophic Factor promotes the maturation of GABAergic mechanisns in cultures hippocampal neurons. J Neurosci 2002; 22: 7580-7585.

39 Deisseroth K, Singla S, Toda H et al. Excitation-neurogenesis coupling in adult neural stem/progenitor cells. Neuron 2004; 42: 535-552.

40 Spitzer NC, Root CM, Borodinsky LN. Orchestrating neuronal differentiation: patterns of Ca^{2+} spikes specify transmitter choice. Trends Neurosc 2004; 27: 415-421.

Figure legends

Figure 1. Experimental design. Embryoid bodies (EBs) were made by culturing ES cells with DMEM containing 10% FCS in non-coated bacterial petri dishes (Nunc). Electrical stimulation was applied to cells in a 4-mm gap cuvette under several voltage conditions (0V, 5V, 10V, and 20V; see supplemental data). For cell culture experiments, stimulated EBs were maintained in DMEM with 10% FCS (GIBCO) on poly-D-Lysine-coated plates (BD). For animal experiments, Venus-positive EBs were stimulated similarly (10 V, same 5-pulse train) and then dissociated with trypsin-EDTA for 3 min. Dissociated cells were injected into C57BL/6 blastocysts.

Figure 2. Effect of electrical stimulation on ES cell differentiation in culture. (**A-D**) Increasing, mild electrical stimulation disproportionately biases ES cell differentiation toward a neuronal fate. Percentage of colonies containing cells that express the neuronal marker TuJ1 (**A**), and those that express the muscle marker α-actinin (**B**). Black filled circles, original ES cells; white open circles, ES cells cultured for 1 d to make embryoid bodies (EBs) (before electrical stimulation); blue filled circles, ES cells cultured for 2 d

to make EBs (before electrical stimulation); and red filled circles, ES cultured for 3 d to make EBs (before electrical stimulation). Number of TuJ1-positive cells per colony (**C**) and α-actinin-positive cells per colony (**D**), both as a function of stimulation intensity. Daggers indicate $p < 0.001$ and asterisks indicate $p < 0.05$ compared to TuJ1-positive cells in zero-volt condition. Statistical differences between groups were assessed with the Student t-test. A p value of at least $p < 0.05$ was considered significant. Numbers in parentheses in (**C**) and (**D**) indicate the number of colonies containing TuJ1-positive cells. (**E-G**) Appearance of unstimulated control EBs. Although the majority of colonies did not contain TuJ1-positive cells (**E**), a few TuJ1-positive cells were present (**G**). (**F**) Nuclear staining of EBs in (**E**) shows the density of cells. (**H-L**) Appearance of stimulated EBs. Anti-TuJ1 immunostaining of EBs subjected to either 5 V (**H**), 10 V (**I**), or 20 V (**J**) pulse stimulation. (**K**) Higher magnification of anti-TuJ1 immunostained EBs stimulated with 10 V. (**L**) Anti-α-actinin immunostained EBs stimulated with 10 V. (**M**) Nuclear staining demonstrates the existence of cells and lack of anti-TuJ1 immunostaining of ES cells. (**N**) Neuronal differentiation of ES cells was

not induced. Nuclear stain was propiodium iodide. Scale bars, 1 mm (**E-G**), 100 μm (**H-J, L**), 500 μm (**K**), and 200 μm (**M, N**).

Figure 3. Electrical stimulation-induced calcium influx into cells. (**A-C**) Changes of $[Ca^{2+}]_i$ in EBs (**A, B**) and in ES cells (**C**) following electrical stimulation. Ratio of fluorescence excitation intensities at 340 nm to 380 nm is plotted as a function of time. Filled arrowheads indicate time of electrical stimulation. Three typical patterns are displayed for each plot. Inset in (**A**) shows a fluorescent image of fura-2-loaded EBs excited at 380 nm. The culture medium contained either 2 mM Ca^{2+} (**A, C**) or 25 mM EGTA (**B**). Cells were stimulated at 30 V (5 to 6 W) in this experiment. Due to the different buffer composition for this experiment, a higher voltage was required to produce comparable power (5-6 W) to that produced in the 10 to 15 V condition of the experiments presented in Figure 1. This stimulus intensity (one associated with 5-6 W) induces neuronal differentiation. (**D**) Mean number of neuronal cells counted per colony in the presence and/or absence of the calcium chelator EGTA and stimulation with electric pulses (EP). The number of neuronal cells decreased dramatically when Ca^{2+}

was absent from the medium. The same stimulation condition that yielded TuJ1-positive cells failed to yield neuronal cells when 25 mM EGTA was added to the medium. Open bars show data for incubation without EGTA and closed bars with EGTA. Number of colonies counted is indicated in parentheses. Again due to the difference in culture conditions in this experiment, cell growth was largely disturbed in comparison with the conditions used in the experiments of Figure 1. The absolute number of cells after culturing was about one-tenth of the number of cells in the experiments presented in Figure 1. Statistical differences between groups were assessed with the Student t-test. Error bars are SEM. $p = 0.00057$ for comparison (*) between stimulated EBs with EGTA present and stimulated EBs with EGTA absent.

Figure 4. Distribution of electrically stimulated ES cells implanted in mouse embryos. An embryo at 11 dpc was sectioned to examine cell-type specificity of incorporated fluorescent ES cells in the CNS. Incorporation of ES cells into brain (**A-C**) and spinal cord (**D-Q**), shown in transverse sections. Green fluorescent puncta are anti-GFP-positive cells expressing Venus (**A, C, D, G, H, K**), red are TuJ1-positive cells,

indicating differentiated neurons (**B, E, G, I, J**), and blue shows nuclear staining with TO-PRO3 (Molecular Probes) (**F, G, J, K**). Small boxes in **D-G** show areas of high magnification presented in **H-K,** respectively. (**L-Q**) High magnification images of a 13 dpc embryo showing that ES cells differentiated into a variety of neuron types, including motor neurons, interneurons, or their precursors. Green signals represent GFP and Red signals, Islet1 (**L-N**), Pax6 (**O-Q**). Scale bars, 500 μm (**A-C**), 250 μm (**D-G**), 50 μm (**H-K**), and 40 μm (**L-Q**).

Figure 5. Longitudinal sections of injured, adult mouse spinal cords injected with electrically stimulated or non-stimulated cells. (**A-D**) Hematoxylin-eosin staining. Injured spinal cords 57 days after trauma was induced without injection of ES cells (control) (**A**). (**B-D**) Untreated or treated ES cells were injected 7days after injury. Histological analysis was done 50 days after injection with unstimulated ES cells (**B**), with non-stimulated EBs (EB) (**C**), or stimulated EBs (electropulsed, EP) (**D**). Scale bar, 1 mm. (**D**) Incorporation of electrically stimulated EBs into injured adult spinal cord.

(**Db**) Cells derived from stimulated EBs (electropulsed; EP) are positive for GFP. (**Dc**) ES cells from stimulated EBs differentiated into Hu-positive neuronal cells.

Figure 6. Stimulated EBs frequently adopted the appearance of neuronal cells when injected into spinal cord. (**A-D**) Almost all the cells derived from stimulated EBs (electropulsed, EP) displayed Hu immunoreactivity but not Ki67 immunoreactivity, whereas cells derived from unstimulated EBs (EB; **E-H**) or ES cells (ES; **I-L**) displayed Ki67 immunoreactivity but not Hu immunoreactivity. (**M**) Graph showing the percentage of cells that co-express both GFP and Hu. (**N**) Graph showing the percentage of cells that co-express both GFP and Ki67. Percentages indicated were average of percentages of Hu or Ki67 positive cell counts obtained by tallying the GFP-positive cells observed in more than 10 different focal planes of each EP, EB and ES examined. Green, blue and red signals indicate GFP, Hu and Ki67 immunoreactivity, respectively (**A-L**). Scale bar, 50 μm.

Figure 7. Stimulated EBs adopted the appearance of various types of neuronal cells when injected into spinal cord. (**A-C**) Almost all the cells derived from stimulated EBs (electropulsed, EP) displayed MAP2 immunoreactivity, indicating that they had differentiated into mature neurons. Some of the cells derived from EPs expressed ChAT, a motor neuron marker (**D-F**), or parvalbumin, an inhibitory neuron marker (**G-I**). Scale bar, 50 μm.

Yamada et al. Figure 1

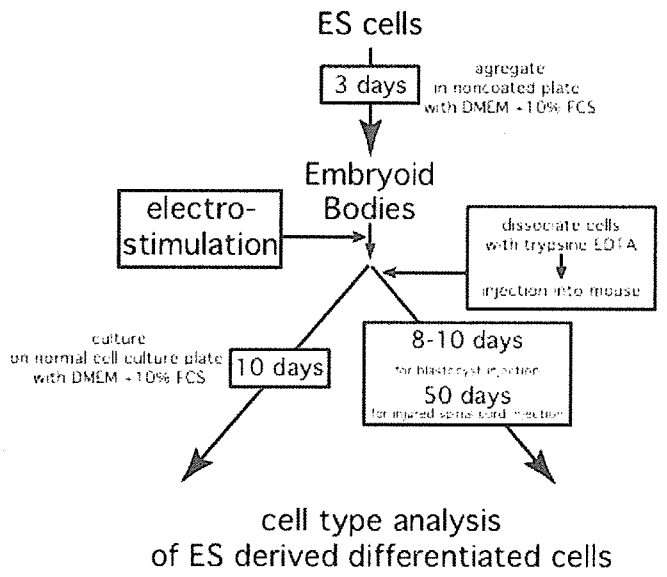

Yamada et al. Figure 2

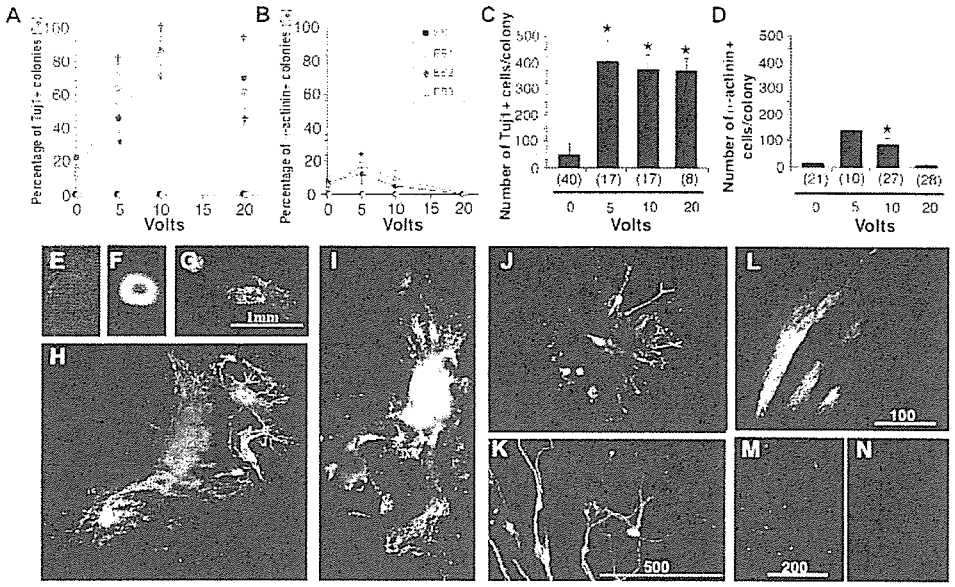

Yamada et al. Figure 3

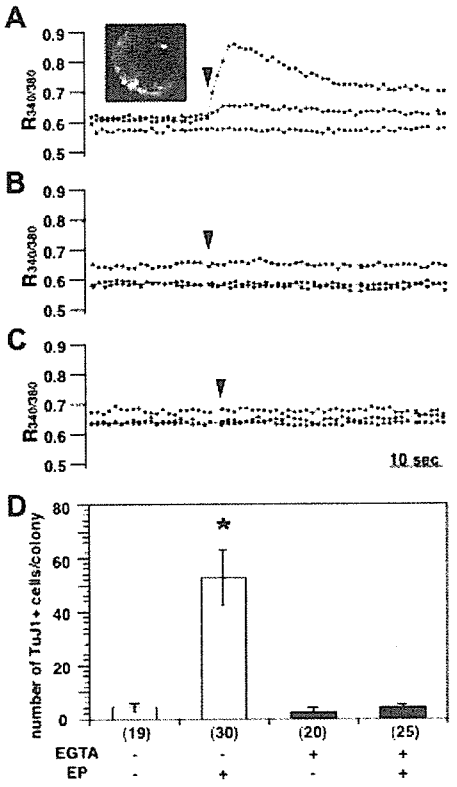

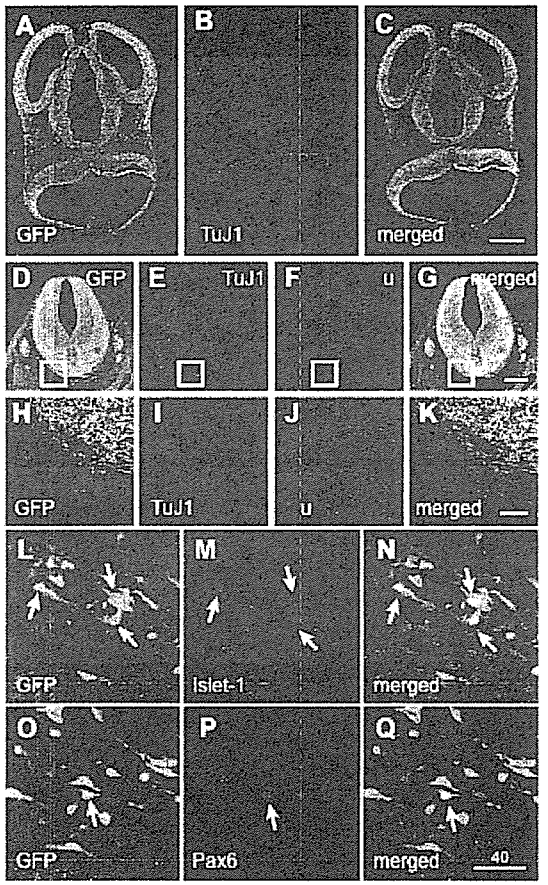

Yamada et al. Fig.5

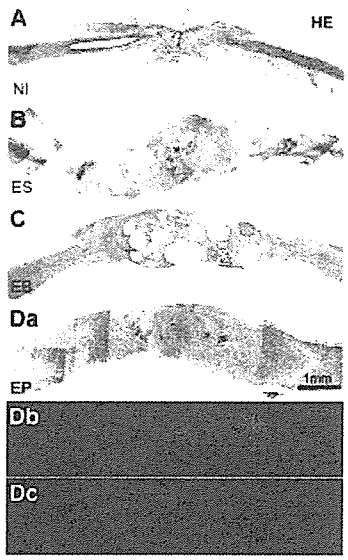

Yamada et al. Fig.6

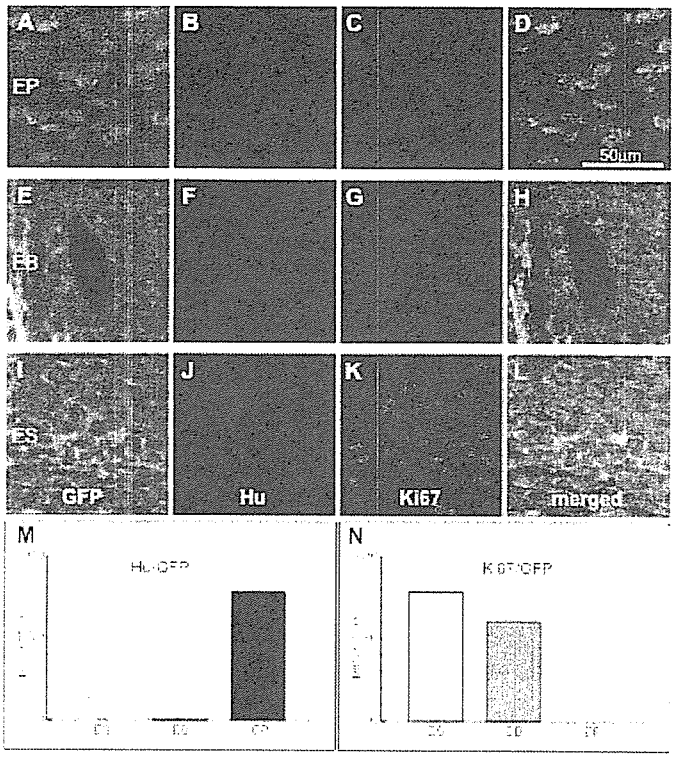

Yamada et al. Fig.7